NONLEPTONIC WEAK DECAYS OF BOTTOM MESONS

by

A. Ali, J. G. Körner, G. Kramer

II. Institut für Theoretische Physik der Universität Hamburg

J. Willrodt

Deutsches Elektronen-Synchrotron DESY, Hamburg

To be sure that your preprints are promptly included in the
HIGH ENERGY PHYSICS INDEX ,
send them to the following address (if possible by air mail) :

Nonleptonic Weak Decays of Bottom Mesons [+]

A. Ali, J.G. Körner, G. Kramer

II. Institut für Theoretische Physik der Universität Hamburg

J. Willrodt [++]

Deutsches Elektronen-Synchroton DESY, Hamburg

Abstract

Based on the Kobayashi-Maskawa weak current model we investigate the properties of weak hadronic decays of the anticipated bottom mesons. Our main results concern twobody and quasi-twobody decays of bottom mesons into pseudoscalar and vector mesons.

1. Introduction

The discovery of Υ (9.46) by Herb et al. [1] and its confirmation in e^+e^--annihilation by two groups working at DORIS [2] make it very likely that a new quark called bottom, b, with charge Q = -1/3 exists. If the usual interpretation of Υ (9.46) as a $\bar{b}b$ bound state is correct, mesons with bottom quantum number B ≠ 0 should also exist. These would consist of bound states of the b quark with the known antiquarks $\bar{u}$, $\bar{d}$, $\bar{s}$ and $\bar{c}$. The lowest lying multiplet of these new bottom mesons must decay weakly. The anticipated discovery of the new mesons has at least two important implications. First, their confirmation would give us evidence that a new quantum number bottomness exists. Second, we would obtain information on the nature of the b quark and in particular on its weak interaction properties.

The favoured model of weak interaction for the b quark is a simple extension of the standard Weinberg-Salam model [3]. To the well-known left-handed doublets one adds the doublet $(t, b)_L$ where the top quark t is the higher lying partner of the **b** with charge 2/3. This six quark model was first discussed by Kobayashi and Maskawa (KM) [4].

Several authors have already investigated some of the anticipated properties of the weak interactions associated with b and t quarks in the context of the KM model [5,6]. In a recent paper we have studied the properties of quark jets originating from the decays of heavy mesons containing b quarks [7]. Unfortunately the masses of the bottom mesons, which are expected to lie in the range 5 - 7 GeV, are not high enough for the decays to exhibit clear 6 quark-jet effects. The weak decays of the b quarks then result mainly in a jet broadening of the original (b + $\bar{b}$) 2 jet configuration, without the second

stage jets from the weak decays becoming discernible. In order to see clear jets from weak decays one will probably have to wait for the production of the next heavy quark, the t-quark. It is, therefore, important to study the hadronic decays of the bottom mesons by looking at specific decay modes and estimate the inelasticity (multipionic and kaonic modes) using some statistical model description.

As a first step towards describing the final hadronic states in the decay of bottom mesons, we evaluate the twobody and quasi two body decay channels. Although the branching ratio into these two body channels is expected to be only a few percent these channels possess a unique structure due to the properties of the KM weak current which predicts that channels with at least one charmed particle or one $c\bar{c}$ state are dominant. This would provide a good signature for the detection of the B-meson. The measurement of these two body rates would also provide a test of the theoretical ideas that go into such a calculation of which the main ingredient is the behaviour of the KM current x current product at short distances. Measurement of the final states with definite quantum numbers in the decay of B mesons would be the cleanest way to determine the mixing angles Θ_2 and Θ_3 .

In section 2 we briefly recapitulate the properties of the KM current and discuss the dominant contributions in the current x current product. Short distance effects are incorporated as usual by hard gluon corrections [8]. The resulting effective Hamiltonian is then applied to the calculation of two body decays of bottom mesons where the relevant transition amplitudes are calculated with the help of the quark-parton model. The methods are similar to those used with some success in the calculation of two body

decays of charmed mesons [9,10,11]. Since the relevant mass scale is even higher for B-meson decays, one expects the quark parton approach and the use of the renormalized effective bottom changing Hamiltonian to work even better in this case.

Section 3 contains a short discussion of our results.

2. Two-Body and Quasi-Two-Body Decays

We begin with a short description of the KM weak Hamiltonian [4]. The non-leptonic Hamiltonian has the usual current x current form which results from the lowest order gauge theory diagrams in the limit $m_w \rightarrow \infty$:

$$\mathcal{H}_{n.\ell.} = \frac{G}{\sqrt{2}} \left(J_\mu J^{\mu +} + \hbar.c. \right) \tag{2.1}$$

In the KM model the current J_μ has the form:

$$J_\mu = \bar{u} \gamma_\mu (1 - \gamma_5) \tilde{d} + \bar{c} \gamma_\mu (1 - \gamma_5) \tilde{s} + \bar{t} \gamma_\mu (1 - \gamma_5) \tilde{b} \tag{2.2}$$

with color indices summed over. $\tilde{d}$, $\tilde{s}$ and $\tilde{b}$ are the eigenstates governing the weak interaction which are related to the strong interaction eigenstates d, s and b by a unitary matrix U which in the KM model has the special form

$$U = \begin{pmatrix} c_1 & -s_1 c_3 & -s_1 s_3 \\ s_1 c_2 & c_1 c_2 c_3 - s_2 s_3 e^{i\delta} & c_1 c_2 s_3 + s_2 c_3 e^{i\delta} \\ s_1 s_2 & c_1 s_2 c_3 + c_2 s_3 e^{i\delta} & c_1 s_2 c_3 - c_2 c_3 e^{i\delta} \end{pmatrix} \tag{2.3}$$

The parameters c_i and s_i ($i = 1,2,3$) are connected with three Euler angles: $c_i \equiv \cos\Theta_i$, $s_i \equiv \sin\Theta_i$. δ is the CP violating phase. In the limit $\Theta_2 = \Theta_3 = 0$ the angle $\Theta_1 = \Theta_c$ is the well-known Cabibbo angle. Unfortunately nothing definite is known about the other angles. Presumably semileptonic decays of B's will be the best source of information for the angle Θ_2 relevant for the decay of the b quark [6]. Theoretical estimates for Θ_2 have been discussed by Ellis et al. [12]. Their estimate is based on the K_L-K_S mass difference. Taking $m_t = 15$ GeV as the mass value for the t quark and $m_c = 1.5$ GeV one arrives at the upper limit $s_2^2 \leqslant 0.06$. The limits for Θ_3 and Θ_1 from the Cabibbo universality are $s_3^2 \leq 0.06$ and $s_1^2 \simeq 0.05$ [12]. In the following we shall restrict ourselves to the terms in (2.1) which are dominant under the above assumptions. They induce the transitions $b \rightarrow cd\bar{u}$ and $b \rightarrow cs\bar{c}$ with coefficients

$$b \rightarrow cd\bar{u} \quad : \quad c_1 (c_1 c_2 s_3 + s_2 c_3 e^{i\delta}) \simeq s_3 + s_2$$

$$b \rightarrow cs\bar{c} \quad : \quad (c_1 c_2 c_3 - s_2 s_3 e^{-i\delta})(c_1 c_2 s_3 + s_2 c_3 e^{i\delta}) \simeq s_3 + s_2$$

(2.4)

We neglect the transitions $b \rightarrow ud\bar{u}$ and $b \rightarrow us\bar{c}$ which are proportional to $s_1 s_3$. In this approximation the non-leptonic Hamiltonian responsible for b transition has the simple form

$$\mathcal{H}_{n.\ell.} = \frac{G}{\sqrt{2}} g_c \left((\bar{c}b)_L (\bar{d}u)_L + (\bar{c}b)_L (\bar{s}c)_L + h.c. \right)$$

(2.5)

where $g_c = s_3 + s_2$ and $(\bar{c}b)_L = \bar{c}\gamma_\mu(1-\gamma_5)b$ etc. Colour summation is implicit in (2.5). The above bare Hamiltonian will be modified by strong interaction effects with the result that the Fierz odd and Fierz even

components of the bare Hamiltonian are multiplicatively renormalized with renormalization constants f_- and f_+, respectively [8]. The corresponding operators transform as 75 and 200 in SU(5). The resulting effective Hamiltonian can then be written as

$$\mathcal{H}^{eff.}_{n.\ell.} = \frac{G}{\sqrt{2}} g_c \left\{ \frac{1}{2}(f_+ + f_-) \left((\bar{c}b)_L (\bar{d}u)_L + (\bar{c}b)_L (\bar{s}c)_L \right) \right.$$
$$\left. + \frac{1}{2}(f_+ - f_-) \left((\bar{c}u)_L (\bar{d}b)_L + (\bar{c}c)(\bar{s}b)_L \right) \right\} \tag{2.6}$$

The renormalization coefficients can be estimated in an asymptotically free theory as in QCD by considering hard gluon exchange effects [8,13]. Since the effective mass scale set by the b-quark mass is higher than in the charmed quark case, the renormalization for b decays is weaker than for c decays [12]. We use the estimate of Ellis et al. [12] and take

$$f_- = 1.4$$
$$f_+ = 0.85 \tag{2.7}$$

The above values for f_- and f_+ are already close to their free quark values $f_+ = f_- = 1$. As we shall see later on, meson decay amplitudes are proportional to either of the two linear combinations $\chi_\pm = (2f_+ \pm f_-)/3$. Using the above numbers one has

$$\chi_+ = 1.03$$
$$\chi_- = 0.10 \tag{2.8}$$

compared to the free quark values $\chi_+ = 1$ and $\chi_- = 1/3$. This means that colour suppressed decays from colour connected diagrams are even more suppressed than in the free quark case, whereas contributions from colour disconnected diagrams are little affected by gluon renormalization.

We shall now turn to the calculation of the two body decays of the bottom mesons. For the four possible B = 1 pseudoscalar mesons we use the notation

$$B_u^- = (b\bar{u}) \; , \; B_d^o = (b\bar{d}) \; , \; B_s^o = (b\hat{s}) \; , \; B_c^- = (b\bar{c}) \tag{2.9}$$

Their mass values are computed by adding the masses of the constituent quarks for which we use

$$m_u = m_d = 0.32 \, GeV \; , \; m_s = 0.48 \, GeV \; , \; m_c = 1.55 \, GeV, \; m_b = 4.7 \, GeV \tag{2.10}$$

Thus we shall use the following mass values

$$M_{B_u^-} = M_{B_d^o} = 5.02 \; GeV$$

$$M_{B_s^o} = 5.18 \; GeV \tag{2.11}$$

$$M_{B_c^-} = 6.25 \; GeV$$

Since gluon exchange effects are taken into account by the effective non-leptonic interaction (2.6) the non-leptonic decay of a heavy bottom meson B is fully described by the diagrams in fig. 1. For the purpose of illustration we have chosen to label the diagrams for the specific channel $B_c^- \rightarrow (c\bar{c}) + (s\bar{c})$ since this particular decay channel has contributions from all three types

of diagrams. In all other cases the number of contributing diagrams is less (or even zero in a few cases). In the latter case one would call such a decay Zweig forbidden.

The full decay amplitude is given by the sum of three factorizing contributions [9] corresponding to Ia, IIa and IIIa in fig. 1. One has for the particular configuration in fig. 1

$$
\langle \eta_c F^- | \mathcal{H}_{n.e.}^{eff} | B_c^- \rangle = \frac{G}{\sqrt{2}} g_c \Big(\tfrac{1}{2}(f_+ - f_-) \langle \eta_c | J_\mu^o | 0 \rangle \langle F^- | J^{\mu o} | B_c^- \rangle
$$

$$
+ \tfrac{1}{2}(f_+ + f_-) \langle F^- | J_\mu^- | 0 \rangle \langle \eta_c | J^{\mu +} | B_c^- \rangle \qquad (2.12)
$$

$$
+ \tfrac{1}{2}(f_+ + f_-) \langle \eta_c F^- | J_\mu^- | 0 \rangle \langle 0 | J^{\mu +} | B_c^- \rangle \Big)
$$

The colour connected diagrams Ib, IIb and IIIb are related to the colour disconnected diagrams Ia, IIa and IIIa as usual by a Fierz transformation. Taking into account colour factors the net result of adding type a colour disconnected and type b colour connected diagrams is that in the neutral current contribution in (2.6) the factor $1/2(f_+ - f_-)$ is replaced by $\chi_- = (2f_+ - f_-)/3$ and in the charged current contribution in (2.6) the factor $1/2(f_+ + f_-)$ is replaced by $\chi_+ = (2f_+ + f_-)/3$.

For the corresponding PV and VV final state we have the analogous sum of factorizing terms as in (2.12) involving current matrix elements containing P or V particles.

Some of the current matrix elements in (2.12) appear also in leptonic and semileptonic decays of B_c^- and F^-, whereas the others can in principle be related to physical leptonic and semileptonic decays using some minimal theoretical input like SU(3) symmetry and crossing. The lack of data for these decays forces us to use theoretical models for them.

Next, we discuss our assumption for the matrix elements $\langle P | J_\mu^- | 0 \rangle$ and $\langle V | J_\mu^- | 0 \rangle$, which have the form:

$$\langle P | J_\mu^- | 0 \rangle = i f_P P_\mu \tag{2.13}$$

$$\langle V | J_\mu^- | 0 \rangle = m_V^2 f_V e_\mu \tag{2.14}$$

The vector meson decay constants are fixed according to the empirical rule that the leptonic widths (or equivalently $(m_V)^{1/2} f_V$) show SU(4) invariance. We therefore take

$$f_V (q_1 \bar{q}_2) = \left(\frac{2 m_u}{m_{q_1} + m_{q_2}} \right)^{1/2} f_{g^+} \tag{2.15}$$

where the dimensionless constant $f_{g^+} = 0.24$.

Since the empirical massbreaking indicated in (2.15) manifests itself in the way the quark wavefunction at the origin is broken, we shall use a mass-breaking formula equivalent to (2.15) for f_p (f_p is determined by the same

quark wave function at the origin). We shall therefore take

$$f_P(q_1\bar{q}_2) = \left(\frac{m_{q_1} + m_{q_2}}{2m_u}\right)^{1/2} f_{\pi^+}$$

(2.16)

with f_{π^+} = 0.13 GeV. This leads to $f_B \approx 0.4$ GeV which is close to the value used by Ellis et al. [12]. Further, we need to specify the structure of the two particle current matrix elements in (2.12). The corresponding charm changing current transition $D \to K (K^*)$ has been treated extensively in the literature [9-11,14-20], although the choice of form factor invariants differs from author to author. We shall use the form factor invariants resulting from the use of U(2,2) quark model wave functions as has been done in the study of Craigie et al. [20]. The U(2,2) approach has the advantage that the calculated amplitudes optimally reflect the helicity structure of the underlying quark dynamics as will be discussed in detail in the following.

We have found it advantageous to evaluate the two body decay amplitudes directly in the quark model from the diagrams in fig. 1, since such a procedure allows one to handle relative phases of various contributions in a consistent manner. Using the U(2,2) quark model wave functions [21], one obtains the following results for the two body decays of an 0^- meson.

Case A $0^- \to 0^- + 0^-$

$$T^I = \left[(P_1 + P_3)_\mu - \frac{(M_1 - M_3)}{(M_1 + M_3)}(P_1 - P_3)_\mu\right]_V \left[i f_{P_2} P_{2\mu}\right]_A Tr(1\Gamma\bar{3} - 1\bar{3}\Gamma)$$

(2.17a)

$$T^{II} = \left[(P_1 + P_2)_\mu - \frac{(M_1 - M_2)}{(M_1 + M_2)} (P_1 - P_2)_\mu \right]_V \left[i f_{P_3} P_{3\mu} \right]_A Tr\,(1\Gamma\bar{2} - 12\Gamma) \qquad (2.17b)$$

$$T^{III} = \left[(P_2 - P_3)_\mu - \frac{(M_2 - M_3)}{(M_2 + M_3)} (P_2 + P_3)_\mu \right]_V \left[i f_{P_1} P_{1\mu} \right]_A Tr\,(\bar{2}\Gamma\bar{3} - \bar{2}\bar{3}\Gamma) \quad (2.17c)$$

Case B $\quad 0^- \rightarrow 0^- + 1^-$

$$T^{I} = i \left[(M_1 + M_3)\bar{e}_{3\mu} - \frac{2}{M_1 + M_3} P_1 \cdot \bar{e}_3 P_{3\mu} \right]_A \left[i f_{P_2} P_{2\mu} \right]_A Tr\,(1\Gamma\bar{3} - 1\bar{3}\Gamma) \qquad (2.18a)$$

$$T^{II} = \left[-(P_1 + P_2)_\mu + \frac{M_1 - M_2}{M_1 + M_2} (P_1 - P_2)_\mu \right]_V \left[M_3^2 f_{V_3} \bar{e}_{3\mu} \right]_V Tr\,(1\Gamma\bar{2} - 1\bar{2}\Gamma) \qquad (2.18b)$$

$$T^{III} = i \left[-(M_2 + M_3)\bar{e}_{3\mu} - \frac{2}{M_2 + M_3} P_2 \cdot \bar{e}_3 P_{3\mu} \right]_A \left[i f_{P_1} P_{1\mu} \right]_A Tr\,(\bar{2}\Gamma\bar{3} - \bar{2}\bar{3}\Gamma)$$
$$\qquad (2.18c)$$

Case C $\quad 0^- \rightarrow 1^- + 1^-$

$$T^{I} = i \left[(M_1 + M_3)\bar{e}_{3\mu} - \frac{2}{M_1 + M_3} P_1 \cdot \bar{e}_3 P_{3\mu} \right]_A \left[M_2^2 f_{V_2} \bar{e}_{2\mu} \right]_V Tr\,(1\Gamma\bar{3} - 1\bar{3}\Gamma)$$
$$\qquad (2.19a)$$

$$\left[-\frac{2}{M_1 + M_3} \epsilon_{\mu abc}\, \bar{e}_{3a} P_{1b} P_{2c} \right]_V \left[M_2^2 f_{V_2} \bar{e}_{2\mu} \right]_V Tr\,(1\Gamma\bar{3} + 1\bar{3}\Gamma)$$

$$T^{II} = i \left\{ (M_1 + M_2) \bar{e}_{2\mu} - \frac{2}{M_1 + M_2} P_1 \cdot \bar{e}_2 P_{2\mu} \right\}_A [M_3^2 f_{V_3} \bar{e}_{3\mu}]_V \, Tr \, (1\Gamma\bar{2} - 1\bar{2}\Gamma) \qquad (2.19b)$$

$$+ \left[\frac{2}{M_1 + M_2} \epsilon_{\mu abc} \bar{e}_{2a} P_{1b} P_{2c} \right]_V [M_3^2 f_{V_3} \bar{e}_{3\mu}]_V \, Tr \, (1\Gamma\bar{2} + 1\bar{2}\Gamma)$$

$$T^{III} = \left[\left(\frac{2}{M_2 + M_3} \right) (-M_2 P_{3\mu} + M_3 P_{2\mu}) e_2 \cdot e_3 + \frac{2(1 + \mu_p^a)}{M_2 + M_3} (M_2 P_3 \cdot \bar{e}_2 \, e_{3\mu} - M_3 P_2 \cdot \bar{e}_3 \, e_{2\mu}) \right]_V$$

$$\times [i f_{P_1} P_{1\mu}]_A \, Tr \, (\bar{2}\Gamma\bar{3} + \bar{2}\bar{3}\Gamma)$$

$$(2.19c)$$

$$+ i \left[- \frac{2M_3}{M_2 + M_3} \epsilon_{ab\mu c} \bar{e}_{2a} \bar{e}_{3b} P_{2c} + \frac{2M_2}{M_2 + M_3} \epsilon_{ab\mu c} \bar{e}_{2a} \bar{e}_{3b} P_{3c} \right]_A$$

$$\times [i f_{P_1} P_{1\mu}]_A \, Tr \, (\bar{2}\Gamma\bar{3} - \bar{2}\bar{3}\Gamma)$$

We have employed a short hand notation for the meson matrices in flavour space such that 1 and $\bar{1}$ denote mesons in the initial and final state, etc. Γ is the current structure in flavour space. The pseudoscalar and vector meson decay constants f_{P_i} and f_{V_i} have been defined in (2.13) and (2.14). They are proportional to the flavour traces $Tr \, (\Gamma P_i)$ and $Tr \, (\Gamma V_i)$, respectively, and are relatively <u>positive</u> for a given state i. In (2.19c) we have included the factor $(1 + \mu_p^a)$, where μ_p^a = 1.87 is the anomalous magnetic moment of the proton [F1]. There are a number of remarks and comments we want to make about the amplitudes (2.17) - (2.19).

We have written our results in a factorized form so as to make the connection with the representation in terms of current matrix elements (2.12) explicit. The factorized contributions have a subscript V or A depending on whether they result from the vector or axial vector part of the current.

As described earlier the contributions of diagrams Ib, IIb and IIIb are

related to Ia, IIa and IIIa via a Fierz transformation. The sum of the two diagrams in such a pair results in the explicit factors $\chi_\pm = 1/3(2f_+ \pm f_-)$ depending on whether the current transition in Ia, IIa, IIIa is charged (χ_+) or neutral (χ_-) (see fig. 1). These factors as well as the explicit weak interaction factors $g_c G/\sqrt{2}$ have not been written out in (2.17) - (2.19).

In fig. 1 we have only drawn half of the 12 diagrams that would in general contribute to a given mesonic decay. The other 6 diagrams result from those in fig. 1 with the sense of quark line rotation reversed. The sums of two diagrams with opposite rotation sense result in the appearance of the two flavour traces in each amplitude in (2.17)-(2.19), which give the appropriate symmetric and antisymmetric D- and F-couplings in flavour space. Since the order of traces is important for the phase of the antisymmetric F-coupling $Tr(\lambda \Gamma \bar{j})$ is to be evaluated in the order $i \to \Gamma \to j$ with the direction given by the quark lines in the appropriate quark diagrams [F2].

Next, we discuss the form factors entering the amplitudes (2.17) - (2.19). To incorporate the q^2-dependence we use power behaved form factors $(1 - q^2/m^2)^{-n}$ For the parameter m, we assume the mass of the mesons having the quantum numbers of the current-channel, with the bottom meson masses taken from (2.11). For the form factor power n, we take the canonical values [24,25] (see appendix). The diagrams III are substantially suppressed due to the form factor effects. This comes about because for these diagrams the scale of q^2 is set by the bottom meson mass and that of m by ordinary or charmed mesons. On the other hand, for diagrams of type I and II, the mass-scale for m is typically that of the bottom mesons while q^2 corresponds to either ordinary meson or charmed meson masses. Thus, for diagrams of type I and II the form factors' effect

is to enhance the contribution of these diagrams, particularly when $q^2 \simeq m_D^2$ etc. and n is large, as is the case involving vector mesons.

Before turning to the quantitative results we would like to discuss some general qualitative features of the decay rates following from the amplitudes (2.17) - (2.19). The relevant large kinematical quantities in the decay process are the energies of the decay products which are proportional to M_1, the mass of the decaying meson. Thus it is appropriate to expand the decay width formulae in powers of M_1. To leading order one obtains [F3]:

PP : $$\Gamma^0 \simeq G^2 M_1^3 f_P^2 \cdot g_c^2 / 32\pi \qquad (2.20)$$

PV : $$\Gamma^0 \simeq G^2 M_1^3 f_P^2 \cdot g_c^2 / 32\pi \qquad \text{diagram I} \quad (2.21a)$$

$$\Gamma^0 \simeq G^2 M_1^3 M_V^2 f_V^2 \cdot g_c^2 / 32\pi \qquad \text{diagram II} \quad (2.21b)$$

VV : $$\Gamma^0 \simeq G^2 M_1^3 M_V^2 f_V^2 \cdot g_c^2 / 32\pi \qquad (2.22a)$$

$$\Gamma^- \simeq 4 G^2 M_1 M_V^4 f_V^2 \cdot g_c^2 / 32\pi \qquad (2.22b)$$

$$\Gamma^+ \simeq 4 G^2 M_1^{-1} M_{V'}^2 M_V^4 f_V^2 \cdot g_c^2 / 32\pi \qquad (2.22c)$$

where $G_F = 1.02 \times 10^{-5} m_p^{-2}$. Γ^0, Γ^- and Γ^+ are longitudinal, transverse negative and transverse positive helicity partial decay widths, respectively. M_p and M_V are pseudoscalar meson and vector meson masses in the final state, and in the VV case $M_{V'}$ denotes the mass of the vector meson occurring in the PV current matrix element.

The leading order structure of the various partial helicity widths in
(2.20) - (2.22) is quite plausible if one turns to the helicity diagrams
depicted in fig. 2. All dominant longitudinal transitions occur via the
contribution fig. 2a and should thus be of the same order in M_1. The trans-
verse negative helicity transition in the VV case occurs through fig. 2c.
Since the heavy quark has to flip its helicity in the interaction one picks
up a kinematical helicity flip suppression factor $(2M_V / M_1)^2$. Finally, the
transverse positive helicity transition occurs via fig. 2d and involves in
addition to the helicity flip suppression factor also the helicity suppression
factor $(M_{V'}/M_1)^2$ since the final quark in the (V-A) interaction appears in
the "wrong" helicity state.

Note that the common power behaviour and the helicity pattern of the widths
(2.20) - (2.22) come about by subtle cancellations among various contributing
U(2,2) form factors. The reasonable final result strengthens our confidence
in the use of the phenomenological U(2,2) quark model wavefunctions. Other
form factors have been suggested in the literature [9,10,11,14] which do not
always lead to the simple structure (2.20) - (2.22) [F4]. For example, the
approaches [6,16,18,19] lead to higher powers of M_1 in the rate formulae
which would result in unreasonably large rates, in particular for the VV
channels.

After this qualitative discussion we now turn to our quantitative predictions
for single channel rates. In table 1 we have listed all possible PP final
states that can be reached with the Hamiltonian (2.6). For the PV and VV
case the corresponding final states can be written down accordingly by making
the appropriate changes in notation. The number of PV final states is double

the number of PP states since either of the two pseudoscalar mesons could be the vector meson. For the η-η' complex we use the usual ($\approx -10^0$) mixing angle [26] and for ω-φ ideal mixing.

According to our previous remarks we expect those single channel rates to be dominant which obtain a χ_+ -contribution from either diagrams I or II. These are made up of the two following classes of transitions

$$B_{q_i} \rightarrow (c\bar{q}_i) + (d\bar{u})$$

(2.23)

and

$$B_{q_i} \rightarrow (c\bar{q}_i) + (s\bar{c})$$

(2.24)

The PP, PV and VV rates of these dominant modes are listed in table 2. The remaining modes are suppressed either by the small factor χ_-^2 (2.8) or by the fact that they occur via diagram III which are small due to form factor effects. In fact, by comparing with the total two body rates in table 3 one sees that the remaining modes constitute only a small fraction of the total two body rate. Of the dominant modes in table 2 one notes that the final states (2.24) involving two heavy charmed mesons are favoured despite their smaller phase space. This is in part due to the massbreaking pattern of the meson decay constants f_p and f_V (2.15) and (2.16) which favours heavy final states. Further the heavy final states are favoured by the time-like form factor effects as discussed above. The most important modes are the final states with two heavy charmed vector mesons of type

$$B_{q_i} \rightarrow (c\bar{q}_i)_V + (s\bar{c})_V \tag{2.25}$$

Relative to their PP and PV counterparts they are enhanced over what one expects from first order asymptotics, viz (2.20), (2.21) and (2.22a), which shows that corrections to the asymptotic formulae are important. For example, the transverse helicity suppression factor $(2M_V/M_1)^2$ is not small in this case and in fact table 2 shows that $\Gamma^- \approx \Gamma^o$ for these enhanced rates. Note that the transverse suppression does hold for the light VV states (2.23). It would be interesting to experimentally check the predicted helicity pattern of the produced VV states. A measurement of the angular distribution of the two pseudoscalar mesons resulting from the decaying D^* or ϱ is sensitive to the ratio $(\Gamma^+ + \Gamma^-)/\Gamma^o$. More involved correlations have to be measured to verify the prediction $\Gamma^- \gg \Gamma^+$.

Let us briefly comment on some of the non-dominant decay channels. A confirmation of the suppression of these modes alone provides a qualitative test of our ideas. A determination of their branching rates, even if difficult experimentally, would provide a more quantitative test of our input assumptions. First, there are the χ_- - contributions that are small because of $(\chi_-/\chi_+)^2 \approx 1\%$. Their rates are very sensitive to the assumed value of the renormalized weak coupling χ_- and thus could occur at a stronger rate if the renormalization were weaker and closer to the free quark value $(\chi_-/\chi_+)^2 = 1/9$. We give some rates which occur at ≈ 1 % level (relative to the rate into that particular two body spin channel) : $B_u^- \rightarrow \eta_c K^- (1.3\%)$; $\Psi K^- (0.7\%)$; $\Psi K^{*-} (2.2\%)$. $B_d^o \rightarrow \eta_c \bar{K}^o (1.6\%)$; $\eta_c K^{*o} (0.8\%)$; $\Psi K^{*o} (2.7\%)$. $B_s^o \rightarrow D^o K^o (1.1\%)$; $K^o D^{*o} (0.8\%)$; $\Psi \varphi (2.7\%)$. $B_c^- \rightarrow D^o D^- (0.8\%)$; $D^o D^{*-} (0.7\%)$; $D^{*o} D^{*-} (0.8\%)$.

Second, there are the B_c^- decay modes which obtain χ_+ - contributions from diagram III and where the form factor mass m is determined by a charmed meson mass as in $B_c^- \to K^- \bar{D}^0$ etc., and where the form factor suppression is thus not so effective. Here we quote $B_c^- \to K^- \bar{D}^0 (K^0 D^-)$ (1.5%);

$F^- \varphi$ (1.2%); $\eta F^- (0.7\%)$; $K^{*-} D^{*0} (K^{*0} D^{*-})(0.7\%)$, where percentage figures again refer to decay rates relative to the relevant spin channel. Establishing these decay modes at the indicated level would test our assumptions about the q^2-behaviour of the form factors, though the branching ratios are prohibitively small.

In table 3 we have listed partial widths of B-mesons going into PP, PV and VV channels as well as the total two-body width. For the sake of comparison we have also calculated the same numbers for the PP channel setting F_- to zero, as has been done e.g. in [6,9]. Note that the magnitude and phase of F_- as calculated using U(2,2) wave functions is in agreement with experiments on $K_{\ell 3}$- decays. However, its contribution to the decays studied here is not very large since the rate is dominated by the contribution of the F_+ form factor. Since F_+ is normalized to 1 as in [6,9] the results are not very different. In the PV and VV case we have also calculated the rates for the two other form factor choices (ii) $F_1^A = 2M_v$, $F_2^A = F^V = F_- = 0$ which is close to [9] and (iii) $F_1^A = M_p + M_v$, $F_2^A = F^V = F_- = 0$ as suggested in [6]. Differences in the results of the three form factor choices can be easily understood by writing out leading order formulae as done in table A1. As already remarked earlier, the form factor choices [6,9] do not reproduce the width structure of (2.20) - (2.22) in every detail as can be verified from table A1.

The total hadronic rate of a bottom meson is usually estimated from the free

quark decay diagram. For the decay $b \rightarrow c + d + \tilde{u}$ one can neglect the masses of the d- and u-quark and obtains

$$\Gamma = \frac{3G^2 M_1^5 g_c^2}{192 \pi^3} F(m_c^2/m_b^2)$$

(2.26)

where $F(x) = 1 - 8x + 8x^3 - x^4 - 12x^2 \ln x$. Using the quark masses (2.10) one has

$$\Gamma_{b \rightarrow c+d+\tilde{u}} = 115 \times 10^{12} \text{ sec}^{-1} g_c^2$$

Note that the rate (2.26) includes a colour factor 3 but not the renormalization factors of the weak current product. As discussed earlier, the free quark limit is a good approximation for estimating inclusive b-decays.

For the decays $b \rightarrow c + s + \bar{c}$ one cannot safely neglect any of the final quark masses. The complete decay formula is too complicated to be reproduced here. Numerically one finds $\Gamma_{b \rightarrow c+s+\bar{c}} / \Gamma_{b \rightarrow c+d+\tilde{u}} \approx 20\%$. Adding the semi-leptonic modes to the above hadronic modes one has for the total decay rate [12,28]

$$\Gamma_B \approx 230 \times 10^{12} \text{ sec}^{-1} g_c^2$$

(2.27)

Compared to the total rate the exclusive rate into two pseudo scalar mesons of the type

$$B_{q_i} \rightarrow (c\bar{q}_i)_P + (d\tilde{u})_P$$

(2.28)

amounts to $\approx 1.5 - 2.0$ %. For decays of type $B_{q_i} \to (c\bar{q}_i)_p + (s\bar{c})_p$ the corresponding percentage figure is $\approx 3 - 5$ %. In fact the two body decays $B_{q_i} \to (c\bar{q}_i) + (s\bar{c})$ in table 3 already tend to oversaturate the rate $\Gamma_{b \to c+s+\bar{c}}$ as calculated in the free quark model. One can probably safely say that in this case the two body channels constitute a significant fraction of that part of the total hadronic rate that is induced by $b \to c + s + \bar{c}$.

It is well known that a similar estimate for the branching rate into two pseudoscalar mesons in charmed meson decays gives too high a value compared to the experimental value ≈ 2 % [23]. We therefore believe that the ≈ 2 % rate calculated for bottom meson decays (2.28) is also too large either for the reason that the total rate is underestimated by (2.27) or else the two body PP rate is overestimated. This could for example happen if there is an additional mass breaking factor in the wave function overlap integral of the current matrix element between pseudoscalar meson states which changes e.g. $F_+ = 1$ to $F_+ = (M_2/M_1)(1+..)$. This question is expected to be settled in the near future when the details of the semileptonic D-decays are disentangled. At any rate, if there were such an additional suppression factor it would equally occur for all the three PP, PV and VV cases since the same overlap is involved in all three cases, and thus our relative rate estimates should still be reliable.

Perhaps a more reliable estimate of the PP branching fraction may be obtained by using scaling arguments appropriate to the powers of M_1 occurring in the exclusive and total width formulae (2.20) and (2.26). Thus, when going from the charm changing to the bottom changing decays one expects the PP rates to decrease by $(m_c/m_b)^2 \approx 0.1$. This would lead us to expect that the bottom meson decay rate into two pseudoscalar mesons is ≈ 0.2 % for $B_{q_i} \to (c\bar{q}_i)_p + (d\bar{u})_p$

decays and $\approx 0.4\%$ for $B_{q_i} \rightarrow (c\bar{q}_\lambda)_P + (s\bar{c})_P$.

3. Discussion

In the preceding section we have estimated the two-body and quasi two-body decay modes of pseudoscalar bottom mesons. We found that all these decay modes add up only to a small fraction of the total decay rate. Our choice of the U(2,2) form factors does, however, enhance the specific two body rates, though the relative rates with respect to specific spin channels are more trustworthy. In particular, we find the two body modes involving a pair of charm meson can have a substantial branching ratio (≈ 1 %). It would be worthwhile to look at the decay modes $B_u^- \rightarrow D^0 F^-$, $(D^{*0}F^- + F^{*-}D^0)$, $D^{*0}F^{*-}$ etc. Implied in the large (≈ 1 %) branching ratio of such decay modes is of course the assumption of the dominance of the $\Delta B = -\Delta C = -\Delta Q$ rule. In this respect our calculation serves to point out the most promising two body decay modes which might be useful for future experiments at PETRA, PEP and CESR.

It is also clear from what has been said in the conclusion of section 2 that an inclusive estimate of the final states in the hadronic decays of the bottom mesons is not very likely to be given by the two body (and quasi two-body) modes. Since the mass of the bottom mesons is still not large enough to justify a three quark jet description of the final hadronic state, a statistical model description seems to be more appropriate. An estimate of the multi body final states (D + multipions, D + K$\bar{K}$ + multipions etc.) and the ensuing hadronic energy distributions etc. is in progress and will be presented elsewhere.

Appendix Kinematical Formulae

We label our momenta by P_1, P_2, P_3 ($P_1 = P_2 + P_3$) where $1 \rightarrow 2 + 3$. In the rest frame of particle 1

$$E_2 = (M_1^2 + M_2^2 - M_3^2)/2M_1$$

$$E_3 = (M_1^2 - M_2^2 + M_3^2)/2M_1$$

$$P_c^2 = E_2^2 - M_2^2 = E_3^2 - M_3^2$$

(A1)

Parity violating amplitudes are denoted by A and p.c. amplitudes by B. We also enumerate the LS amplitudes Γ_{LS} .

Case A $0^- \rightarrow 0^- + 0^-$

L.S. Ampl.: $\Gamma_{00}^{P.V.}$

Inv. Ampl.: $\langle P_2, P_3 | \mathscr{H} | P_1 \rangle = A$ (A2)

$$\Gamma = \frac{1}{8\pi M_1^2} P_c |A|^2$$

(A3)

Case B $0^- \rightarrow 0^- + 1^-$

L.S. Ampl.: $\Gamma_{01}^{P.C.}$

Inv. Ampl.: $\langle P_2, P_3 | \mathscr{H} | P_1 \rangle = \bar{e}_{3\mu} P_{1\mu} B$ (A4)

$$\Gamma = \frac{1}{8\pi M_3^2} P_c^3 |B|^2$$

(A5)

Case C $0^- \rightarrow 1^- + 1^-$

L.S. Ampl.: $\Gamma_{11}^{p.c.}$, $\Gamma_{00}^{p.v.}$, $\Gamma_{22}^{p.v.}$

Inv. Ampl.: $\langle P_2, P_3 | \mathcal{H} | P_1 \rangle = \bar{e}_{3\mu} \bar{e}_{2\nu} (A_1 g_{\mu\nu} + A_2 P_{1\mu} P_{1\nu} + i B \epsilon_{\mu\nu\sigma\delta} P_{1\sigma} P_{2\delta})$

$$(A6)$$

Helicity Ampl.: $H_{00} = \frac{1}{M_2 M_3} \left(\frac{1}{2} (M_1^2 - M_2^2 - M_3^2) A_1 + M_1^2 p_c^2 A_2 \right)$

$$H_{--} = A_1 - M_1 p_c B$$

$$(A7)$$

$$H_{++} = A_1 + M_1 p_c B$$

$$\Gamma = \Gamma^0 + \Gamma^- + \Gamma^+$$

$$= \frac{1}{8\pi M_1^2} p_c \left(|H_{00}|^2 + |H_{--}|^2 + |H_{++}|^2 \right) \qquad (A8)$$

In the main text we are frequently referring to amplitudes occurring in the semileptonic decays $0^- \rightarrow 0^- + \ell + \nu$ and $0^- \rightarrow 1^- + \ell + \nu$.

We define

$$\langle 0^-(P_2) | V_\mu | 0^-(P_1) \rangle = F_+ (P_1 + P_2)_\mu + F_- (P_1 - P_2)_\mu$$

$$(A9)$$

and

$$\langle 1^-(P_2) | A_\mu + V_\mu | 0^-(P_1) \rangle = \bar{e}_{2\nu} (F_1^A g_{\mu\nu} + F_2^A P_{1\mu} P_{1\nu} + i F^V \epsilon_{\mu\nu\sigma\delta} P_{1\sigma} P_{2\delta}) \qquad (A10)$$

The differential decay rate for $0^- \to 0^- + \ell + \nu$ is given by

$$\frac{d\Gamma}{dq^2} = \frac{G^2}{(2\pi)^3} \frac{p^3}{3} |F_+|^2$$

(A11)

and for $0^- \to 1^- + \ell + \nu$ by

$$\frac{d\Gamma}{dq^2} = \frac{G^2}{(2\pi)^3} \frac{q^2 \cdot p}{12 M_1^2} \left(|h_0|^2 + |h_-|^2 + |h_+|^2 \right)$$

(A12)

where one has for the transverse helicity amplitudes

$$h_- = F_1^A - M_1 p \bar{F}^V$$

$$h_+ = F_1^A + M_1 p F^V$$

(A13)

and for the longitudinal helicity amplitude

$$h_0 = (q^2)^{-1/2} \frac{1}{M_2} \left(\frac{1}{2} (M_1^2 - M_2^2 - q^2) F_1^A + M_1^2 p^2 F_2^A \right)$$

(A14)

p denotes the momentum of particle 2 in the rest system of particle one and is given by

$$p^2 = E_2^2 - M_2^2$$

(A15)

where

$$E_2 = (M_1^2 + M_2^2 - q^2)/2M_1$$

(A16)

Canonical form factor powers are n = 1 for $F_\pm$ and F_1^A, and $n = 2$ for F_2^A and F^V (see e.g. [25]). In the contribution of diagram III in the VV case one has the matrix element $\langle V | A_\mu + V_\mu | V \rangle$. In that case the canonical power for the invariant projected out by $g_{ab}(P_1 + P_2)_\mu$ is n = 2 and n = 3 for the others.

For nonzero lepton masses there would be an additional term multiplying e.g. $q_\mu P_{1\nu}$ in (A10). Although the corresponding contribution vanishes in semileptonic decays when the lepton mass is zero this term does in general contribute to the factorized nonleptonic amplitudes. For example, in the case of P → PV one is projecting out the 0^- configuration in the q^2-channel which gives zero contribution to semileptonic decays. It is therefore nontrivial that the U(2,2) approach predicts that there are only the three form factors listed in (A10).

In table R1 we have listed the leading order contributions to the helicity amplitudes in the P→V case for the three models discussed in the main text.

Footnotes

(F1)   The value μ_ρ^a = 1.87 brings the magnetic moment value for the
        vector meson   into   agreement with the
        value predicted by the $SU(2)_W$ scheme [22].

(F2)   The amplitudes in (2.17) - (2.19) are explicitly Bose symmetric
        under exchanges in direct and crossed channels, where one has to
        remember to take $P_i \rightarrow -P_i$ when crossing.

(F3)   We have not written down the leading order expressions for diagrams
        III since they are down by several orders in M_1 due to form factor
        effects discussed above.

(F4)   The same structure is implicitly realized also in the approach of [15].
        The suppression of Γ^+ is also present in [17,18,19].

References

1. Herb S.W. et al.: Phys. Rev. Lett. $\underline{39}$, 252 (1977)

2. Berger Ch. et al.: Phys. Lett. $\underline{76B}$, 243 (1978)
   Darden C.W. et al.: Phys. Lett. $\underline{76B}$, 246 (1978)

3. Weinberg S.: Phys. Rev. Lett. $\underline{19}$, 1364 (1967), Phys. Rev. $\underline{D5}$,
   1412 (1972); Salam A.: Proceedings of the 8th Nobel Symposium
   (Almquist and Wiksells, Stockholm 1968)

4. Kobayashi M., Maskawa K.: Prog. Theor. Phys. $\underline{49}$, 652 (1973)

5. Ellis J., Gaillard M.K., Nanopoulos D.V., Rudaz S.:
   Nucl. Phys. $\underline{B131}$, 285 (1977)
   Carlson C.E., Suya R.: Phys. Rev. Lett. $\underline{39}$, 908 (1977)
   Rizzo T.G.: University of Rochester Report UR-653

6. Ali A.: CERN Report TH 2411, Z. f. Physik C (to be published)

7. Ali A., Körner J.G., Kramer G., Willrodt J.: DESY Report 78/44

8. Lee B.W., Gaillard M.K.: Phys. Rev. Letters $\underline{33}$, 108 (1974)
   Altarelli G., Maiani L.: Phys. Letters $\underline{52B}$, 351 (1974)

9. Fakirov D., Stech B.: Nucl. Phys. $\underline{B133}$, 315 (1978)

10. Cabibbo N., Maiani L.: Physics Letters $\underline{73B}$, 418 (1978)

11. Maiani L.: INFN Preprint Rome (1978)

12. Ellis J., Gaillard M.K., Nanopoulos D.V., Rudaz S.:
    Nucl. Phys. $\underline{B131}$, 285 (1977)

13. Ellis J., Gaillard M.K., Nanopoulos D.V.: Nucl. Phys. $\underline{B100}$, 313 (1975)

14. Ali A., Yang T.C.: Phys. Letters 65B, 275 (1976)

15. Barger V., Phillips R.J.N.: Phys. Rev. D14, 80 (1976)

16. Kane, G.L.: Phys. Letters 70B, 227 (1977)

17. Bletzacker F., Nieh H.T., Soni A.: Phys. Rev. D16, 732 (1977)

18. Nabavi R., Pham X.Y., Cottingham W.N.: J. of Phys. G3, 1485 (1977)

19. Pham X.Y., Richard J.M.: Nucl. Phys. B138, 453 (1978)

20. Craigie N.S., Jones H.F., Milani P.: Imperial College Preprint
    ICTP/77-78/12 (1978)

21. Delbourgo R., Salam A., Strathdee J.: Proc. Roy. Soc. A278,
    146 (1965); Gudehus T.: DESY Report No. 68/11 (1968)
    unpublished; Phys. Rev. 184, 1788 (1969)

22. Gilman F.J., Karliner I.: Phys. Rev. D10, 2194 (1974)

23. Particle Data Group: Phys. Letters 75B, (1978)

24. Amati O., Jengo R., Rubinstein H.R., Veneziano G., Virasoro M.A.:
    Phys. Lett. 27B, 38 (1968)

25. Körner J.G., Kuroda M., Schierholz G.: Phys. Letters 70B, 106 (1977)

26. Isgur N.: Phys. Rev. D12, 3770 (1975); Phys. Rev. D13, 122 (1976)

	I	II	III		I	II	III
$B_u^- \to D^0\pi^-$:	χ_-	χ_+	-	$B_s^0 \to F^+\pi^-$:	-	χ_+	-
D^0F^-:	-	χ_+	-	F^+F^-:	-	χ_+	χ_-
$\eta_c K^-$:	χ_-	-	-	D^0K^0:	χ_-	-	-
				$\eta_c\eta$:	χ_-	-	-
$B_d^0 \to D^+\pi^-$:	-	χ_+	χ_-	$\eta_c\eta'$:	χ_-	-	-
D^+F^-:	-	χ_+	-	D^+D^-:	-	-	χ_-
$D^0\pi^0$:	χ_-	-	χ_-	$D^0\bar{D}^0$:	-	-	χ_-
$D^0\eta$:	χ_-	-	χ_-				
$D^0\eta'$:	χ_-	-	χ_-	$B_c^- \to \eta_c\pi^-$:	-	χ_+	-
$\eta_c\bar{K}^0$:	χ_-	-	-	$\eta_c F^-$:	χ_-	χ_+	χ_+
$\eta_c D^0$:	-	-	χ_-	$\pi^-\pi^0$:	χ_-	-	χ_+
D^+K^-:	-	-	χ_-	K^0K^-:	-	-	χ_+
				$K^-\bar{D}^0$:	-	-	χ_+
				K^0D^-:	-	-	χ_+
				ηF^-:	-	-	χ_+
				$\eta'F^-$:	-	-	χ_+
				$F^-\eta_c$:	-	-	χ_+

Table 1: Decays P → PP with indication of the contributions of diagrams I, II and III in fig. 1. $\chi_\pm$ are the colour-flavour factors (2.8).

PP			PV		VV		(0;-;+)
B_u^- →	$D°\pi^-$:	4.16	$D°S^-$:	7.34	$D^{*°}S^-$:	9.72	(81;17;2)
	$D°F^-$:	8.00	$\pi^- D^{*°}$:	4.29	$D^{*°}F^{*-}$:	28.86	(45;45;10)
			$D°F^{*-}$:	7.67			
			$F^- D^{*°}$:	4.54			
$B_d°$ →	$D^+\pi^-$:	2.72	D^+S^- :	5.48	$D^{*+}S^-$:	6.88	(87;11;2)
	D^+F^- :	6.99	$\pi^- D^{*+}$:	2.68	$D^{*+}F^{*-}$:	25.28	(47;42;11)
			D^+F^{*-} :	6.59			
			$F^- D^{*+}$:	4.34			
$B_s°$ →	$F^+\pi^-$:	3.03	F^+S^- :	5.95	$F^{*+}S^-$:	6.88	(87;11;2)
	F^+F^- :	7.36	$\pi^- F^{*+}$:	2.85	$F^{*+}F^{*-}$:	26.38	(47;41;12)
			F^+F^{*-} :	7.15			
			$F^- F^{*+}$:	4.35			
B_c^- →	$\eta_c\pi^-$:	4.47	$\eta_c S^-$:	8.97	ψS^- :	9.03	(88;10;2)
	$\eta_c F^-$:	17.26	$\pi^-\psi$:	3.79	ψF^{*-} :	49.31	(46;42;12)
			$\eta_c F^{*-}$:	20.65			
			$F^-\psi$:	7.32			

Table 2: Prominent decay modes. Units are $g_c^2 \times 10^{12}$ sec^{-1}. Last column contains percentage of decay into longitudinal, negative and positive helicity states of VV final state.

		PP	PV	VV	Σ
B_u^-	(i)	12.32	24.12	39.47	75.91
	(ii)	14.25	23.84	21.22	59.31
	(iii)	14.25	45.70	75.14	135.09
B_d^o	(i)	9.99	19.60	33.41	63.00
	(ii)	11.74	19.33	17.39	48.46
	(iii)	11.74	34.91	56.47	103.12
B_s^o	(i)	10.70	20.87	34.56	66.13
	(ii)	12.18	20.29	18.79	51.26
	(iii)	12.18	35.56	57.80	105.54
B_c^-	(i)	22.63	42.87	59.85	125.35
	(ii)	23.69	38.45	35.40	97.54
	(iii)	23.69	56.44	86.20	166.33

Table 3: Partial decay widths into PP, PV and VV channels. Fourth column contains total rate. Units are $g_c^2 \times 10^{12} \, \text{sec}^{-1}$. (i) this calculation using $U(2,2)$ form factors (ii) $F_- = 0$, $F_1^A = 2M_v$, $F_2^A = F^V = 0$, $T^{III} = 0$ as in [9] (iii) $F_- = 0$, $F_1^A = M_p + M_v$, $F_2^A = F^V = 0$, $T^{III} = 0$ as in [6].

Table A1: Leading order contributions to helicity amplitudes resulting from different choices for $\langle 1^- | A_\mu + V_\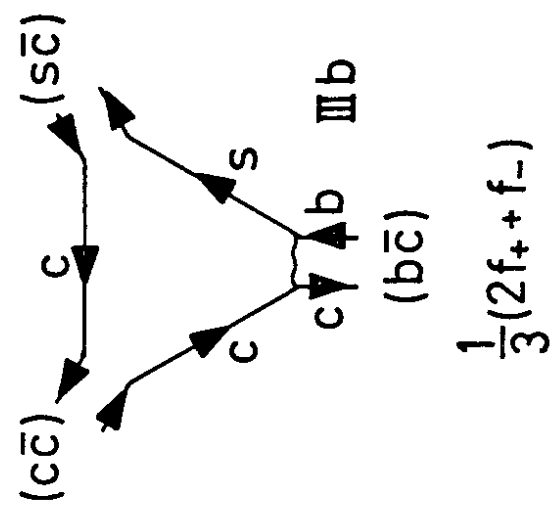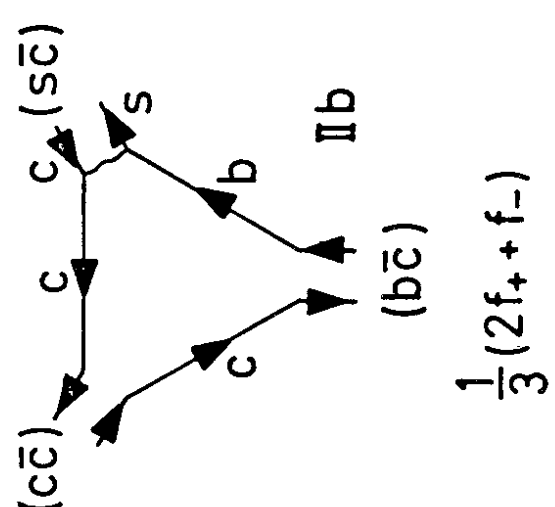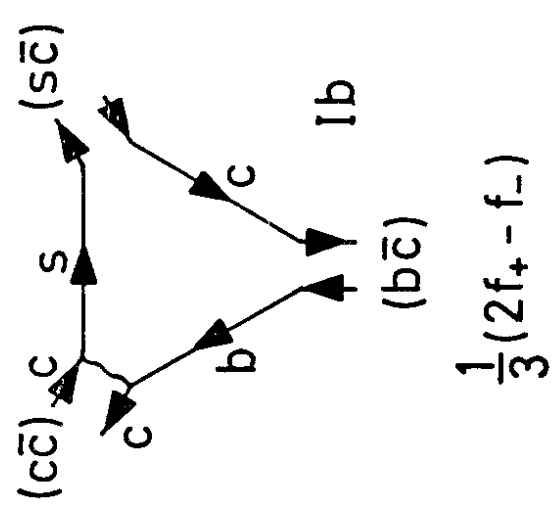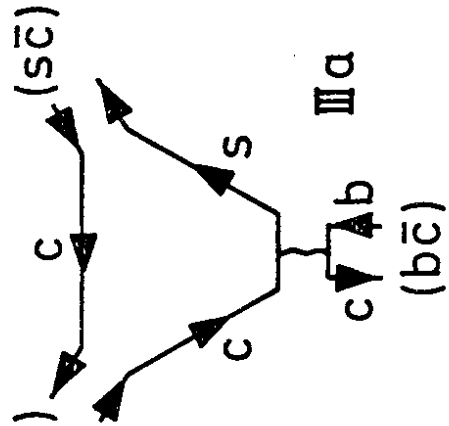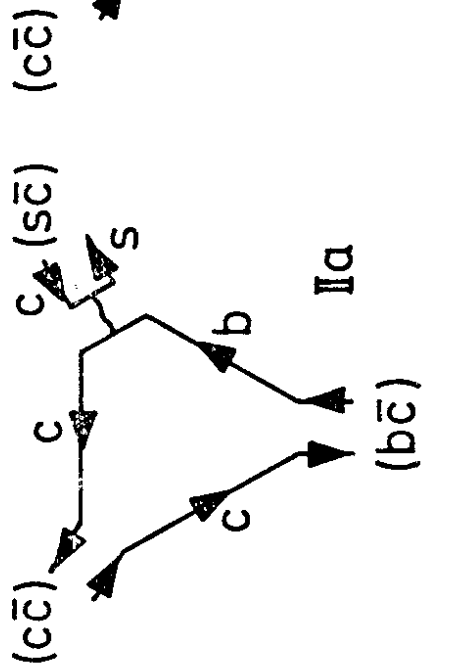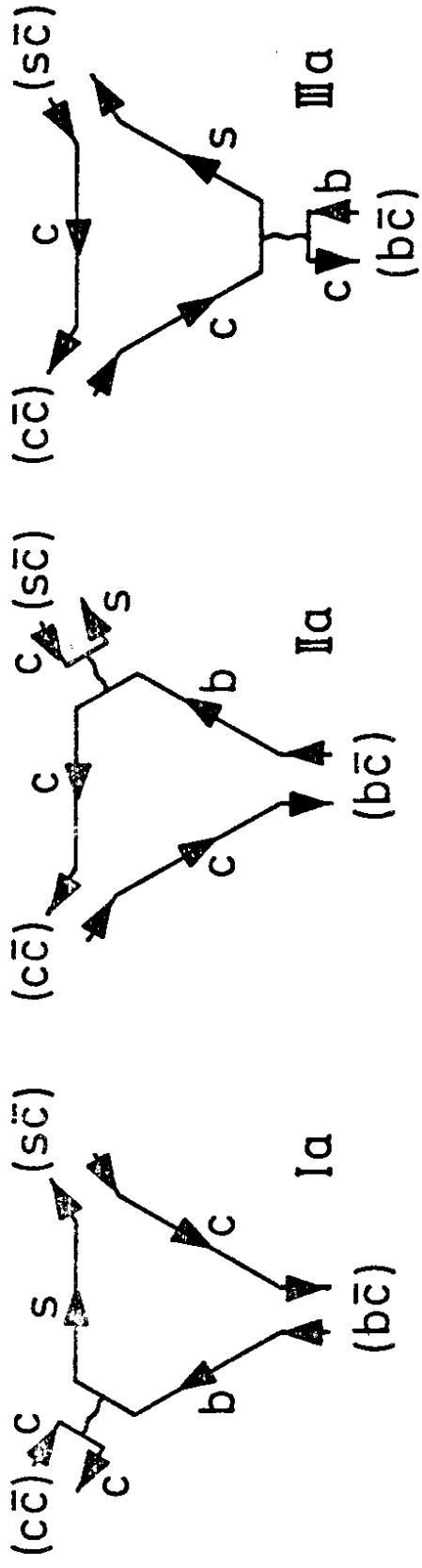mu | 0^- \rangle$ matrix element. (i) U(2,2) $F_1^A = M_P + M_V$, $F_2^A = -2(M_P + M_V)^{-1}$, $F^V = -2(M_P + M_V)^{-1}$ and (ii) $F_1^A = 2M_V$ and (iii) $F_1^A = M_P + M_V$ with $F_2^A = 0$, $F^V = 0$.

	h_0/M_p	h_-/M_p	h_+/M_p
(i)	$M_p/\sqrt{q^2}$	2	$2M_V/M_p$
(ii)	$M_p/\sqrt{q^2}$	$2M_V/M_p$	$2M_V/M_p$
(iii)	$M_p^2/M_V\sqrt{q^2}$	1	1

Figure Captions

Fig. 1:   Quark model decay diagrams. Diagrams are labelled

for the specific decay $B_c^- \rightarrow (c\bar{c}) + (s\bar{c})$.

Fig. 2:   Helicity diagrams. Initial 0^- meson is at rest and appears

at top left of helicity diagrams.

Fig. 1

Ia

Ib
$$\frac{1}{3}(2f_+ - f_-)$$

IIa

IIb
$$\frac{1}{3}(2f_+ + f_-)$$

IIIa

IIIb
$$\frac{1}{3}(2f_+ + f_-)$$

$$H_{oo}$$
$(V-A)$ fav.
no flip
a)

$$H_{oo}$$
$(V-A)$ suppr.
no flip
b)

$$H_{--}$$
$(V-A)$ fav.
flip
c)

$$H_{++}$$
$(V-A)$ suppr.
flip
d)

Fig·2